GPS L5 receiver implementation issues

Christophe Macabiau, Lionel Ries, Frédéric Bastide, Jean-Luc Issler

GPS L5 Receiver Implementation Issues

Christophe MACABIAU, *ENAC*
Lionel RIES, *CNES*
Frédéric BASTIDE, *ENAC/TéSA*
Jean-Luc ISSLER, *CNES*

BIOGRAPHY

Christophe Macabiau graduated as an electronics engineer in 1992 from ENAC (Ecole Nationale de l'Aviation Civile) in Toulouse, France. Since 1994, he has been working on the application of satellite navigation techniques to civil aviation. He received his Ph.D. in 1997 and has been in charge of the signal processing lab of the ENAC since 2000.

Lionel Ries is a Navigation Engineer in the Radionavigation Departement at CNES (French Space Agency), since June 2000. He studies GNSS2 signal including BOC and GPSIIF-L5. In addition, he is involved in experiments on a GNSS2 navigation payload demonstrator (developed by CNES). He formely worked for Altran, as consultant (Astrium, Toulouse and Allgon Stockholm, Sweden). He graduated in 1997 from the "Ecole Polytechnique de Bruxelles, at Brussels Free University (Brussels, Belgium), in 1997, and received a M.S. degree from the "Ecole Nationale Superieure de l'Aeronautique et de l'Espace" (Supaero, Toulouse, France).

Frederic Bastide graduated as an electronics engineers at the ENAC, the French university of civil aviation, in 2001, Toulouse. He is now a Ph.D student at the ENAC. His researches focus on the study of dual frequencies receivers for civil aviation use. Currently he is working on DME/TACAN signals impact on GNSS receivers. He also spent 6 months at the Stanford GPS Lab earlier this year as an exchange researcher.

Jean-Luc Issler is head of the Radio Navigation Department at CNES, whose main task are signal processing and radio-navigation equipments. He is involved in the development of several GNSS spaceborne receivers in Europe, as well as studies on the future European RadioNavigation Programs, like Galileo and the pseudolite network.

ABSTRACT

The new L5 signal is QPSK–modulated, with a nominal carrier frequency of 1176.45 MHz and a bandwidth of 24 MHz. Its two components have each a different spreading code clocked at 10.23 MHz. The in-phase component, also called the data channel, carries the navigation message at 100 symbols per second (50 bits per second with a convolutional encoder) while the quadrature component, called the pilot channel, carries no message at all. The data and pilot L5 spreading codes are each modulated with a distinct Neumann-Hoffman code clocked at 1kHz. The specified power is such that the received levels on the ground should be –154.9 dBW (i.e. –157.9 dBW for each component).

Such a new signal structure implies new receiver structures for acquisition, tracking and data demodulation. In particular, different strategies can be envisioned for L5 codes and Neumann-Hoffman acquisition, and several correlator outputs using data and pilot signals can be combined to form the tracking loops discrimination functions.

The aim of the proposed paper is to show results of an analysis of the possible structures for acquisition of the L5 codes and of the Neumann-Hoffman codes, as well as structures used for L5 signal tracking, and evaluated performance of these acquisition and tracking structures.

I. INTRODUCTION

The US declared in 1999 their intention to provide a new GPS signal called L5 [Spilker and Van Dierendonck, 1999] centred in 1176.45 MHz, targeted for civil aviation uses. That new signal civil should be radiated by the first Block IIF satellites launched in 2005. It will make GPS provide a navigation service more robust for multiple applications, and especially for civil aviation applications. Indeed, this addition will increase Signal-In-Space accuracy, availability, integrity and continuity of service.

This new L5 signal is QPSK–modulated, with a nominal carrier frequency of 1176.45 MHz and a bandwidth

of 24 MHz. Its two components have each a different spreading code clocked at 10.23 MHz. The in-phase component, also called the data channel, carries the navigation message at 100 symbols per second (50 bits per second with a convolutional encoder) while the quadrature component, called the pilot channel, carries no message at all. The data and pilot L5 spreading codes are each modulated with a distinct Neumann-Hoffman code clocked at 1kHz. The specified power is such that the received levels on the ground should be –154.9 dBW (i.e. –157.9 dBW for each component).

Such a new signal structure implies new receiver structures for acquisition, tracking and data demodulation. In particular, different strategies can be envisioned for L5 codes and Neumann-Hoffman acquisition, and several correlator outputs using data and pilot signals can be combined to form the tracking loops discrimination functions.

This paper reports the analysis of several questions raised during the design and the implementation of an L5 generator/receiver simulator carried out by M3SYSTEMS and TéSA (ENAC, SupAéro) for the CNES. Those questions are related to the performance of the acquisition of the L5 and Neumann-Hoffman codes, and to the performance of the different tracking strategies that can be envisioned.

The paper starts by recalling the GPS L5 signal structure and proposed generic receiver architecture. This is followed by two distinct sections, one dealing about acquisition, the second one dealing about tracking.

The classical structure for L5 code acquisition using pilot only or pilot+data channels is described, and acquisition performance is recalled. Next, we describe a proposed technique to acquire the Neumann-Hoffman codes after the L5 codes were acquired, which consists in running an FLL to reduce residual Doppler, then performing a Neumann-Hoffman code search. It is also shown that a FLL can be run after the L5 code acquisition as its loss of lock threshold is below the L5 code acquisition threshold. Finally, we analyze the performance of a proposed structure for direct and combined L5 code and Neumann-Hoffman code acquisition, and we show that its performance is highly degraded when the residual Doppler is larger than 20 Hz. Indication of possible performance improvement using other 10 or 20 bit code will be given in the paper.

We then analyze several possible techniques for code and carrier phase tracking using pilot and data correlator outputs. In particular, concerning carrier phase tracking, we show the analysis of a proposed technique combining data arctangent discriminator and pilot extended arctangent, which requires carrier phase jumps detection and repair, and we show that its performance is no better than the performance of pilot extended arctangent only. A selection of the most appropriate code and phase tracking techniques is finally proposed.

II. GPS L5 SIGNAL STRUCTURE

The L5 signal radiated by satellite *i* is a QPSK modulation of the L5 carrier with a data and a pilot channel that can be modeled as:

$$S_{L5}^{i}(t) = \sqrt{P}\,d^{i}(t)\,NH_{10}(t)\,XI^{i}(t)\cos\left(2\pi f_5 t\right) + \sqrt{P}\,NH_{20}(t)\,XQ^{i}(t)\sin\left(2\pi f_5 t\right)$$

where

- P is such that the minimum total power of the received L5 signal is –154.9 dBW, or –157.9 dBW for each one of the data and pilot component [RTCA, 2000].
- d is the P/NRZ/L materialization of the L5 navigation message encoded with a convolutional FEC (rate ½). The original L5 navigation message has a 50 bps rate, while d has a final 100 sps rate after encoding. Thus the duration of one final symbol in d is 10 ms.
- NH_{10} and NH_{20} are respectively the P/NRZ/L materialization of a 10 bit and 20 bit Neumann-Hoffman code. These codes are clocked at a rate of 1 kHz, thus the duration of one bit is 1 ms.
- XI and XQ are respectively the P/NRZ/L materialization of the data and pilot component PRN codes. Those codes are clocked at a rate of 10.23 MHz and have a period of 1 ms.

Properties of the L5 codes were analyzed in [Macabiau et al., 2002].

III. RECEIVER ARCHITECTURE

The proposed L5 generic receiver tracking loops architecture is shown in figure 1 at the end of this paper.

In each channel, the phase and code tracking loops can potentially use correlator outputs from the data and pilot channels. As a consequence from this, the channel may track the data or the pilot signal or both.

IV. ACQUISITION STRUCTURE /PERFORMANCE

GPS L5 signal acquisition is understood here as the rough synchronization of the signals generated locally by the receiver with the incoming signals. This concerns the local carrier and the local codes. The local codes can be the L5 codes only, or the L5 codes and the Neumann-Hoffman codes.

In this section, we first present a proposed structure for L5 codes acquisition and discuss the performance of this acquisition.

Then, we report the strategies for a complete acquisition of the L5 signal, i.e. the acquisition of the carrier, L5 codes and Neumann-Hoffman codes.

IV.1 L5 CODES ACQUISITION

The L5 codes acquisition is accomplished using both the data and pilot components to use the maximum signal power, as shown in figure 2.

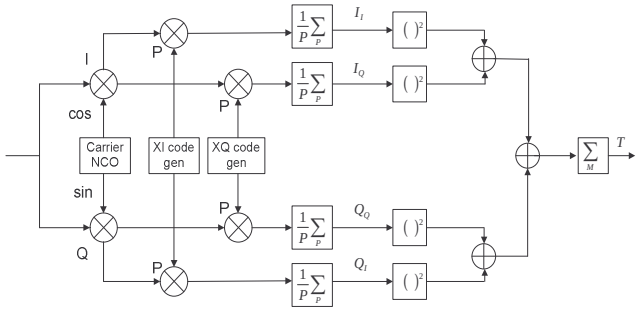

Figure 2: *L5 acquisition structure.*

It has been shown in [Bastide et al., 2002] that an acceptable acquisition threshold with a simple single dwell procedure is around 33.7 dB Hz. This has been obtained through a coherent integration time T_p of 1ms to reduce the Doppler uncertainty bin to a width of [-250 Hz; + 250 Hz] and 15 non-coherent integrations, inducing a worst case loss of -1.5 dB and a mean sequential acquisition time around 164 s when searching only one Doppler bin with a code search step of 0.5 chip. In the case of FFT acquisition, the 33.7 dB acquisition is still valid with T_p=1ms and 15 non-coherent integrations. Note that this threshold is 2dB higher than in the case where only one single data or pilot component is used [Bastide et al., 2002].

The L5 mean code acquisition time is 10 times larger than that the GPS L1 C/A code acquisition time because the L5 codes are 10 times longer than L1 C/A codes and can only be compensated by augmented hardware.

The L5 acquisition performance is also reduced compared to L1 acquisition performance because of the presence of Neumann-Hoffman codes both on the data and pilot signal components. Indeed, these Neumann-Hoffman codes are viewed as data modulation during the acquisition procedure where bit synchronization is not achieved yet. As the length of one Neumann-Hoffman bit is 1 ms, the coherent integration time is therefore limited to 1 ms with L5 to limit power losses due to data bit transitions, while the coherent integration time is limited to 20 ms with L1. Although increasing the coherent integration time has the drawback to increase the number of searched Doppler bins by the same amount, there is an interest to increase that time when only one Doppler bin needs to be searched [Bastide et al., 2002] or when the available hardware has an increased performance. But unfortunately there is no potential improvement of the coherent integration time with L5 from the classical 1ms, which is not the case for L1 C/A.

IV.2. L5 CODES + NEUMANN-HOFFMAN CODES ACQUISITION

Before using correlator samples that have been integrated over an interval larger than 1ms, it is necessary to perform the Neumann-Hoffman codes synchronisation.

That operation can be done using the 1ms samples through a search process similar to the L5 code search process: the 1ms samples are correlated with a local NH code generation and the peak is searched. The problem here is that the search process is affected by the presence of a residual Doppler shift on the 1ms outputs. Therefore, the NH autocorrelation properties are highly degraded because the NH codes are short codes.

As an example, figure 3 shows the signal processing technique proposed in [Hegarty, Tran and Van Dierendonck, 2002] for direct combined NH and L5 code acquisition of the pilot component. The current paper focuses on the degradation of the acquisition criterion used in presence of residual Doppler shift.

The proposed acquisition technique can be applied either on the data or on the pilot signal component.
The input signal (data or pilot component) is expressed as

$$s(t) = \sqrt{P}\,d(t-\tau)c(t-\tau)NH(t-\tau)\cos(2\pi f_0 t - \theta) + n(t)$$ w

here

- P is the L5 signal power (data plus pilot)
- d is the L5 data waveform if the considered L5 component is the data component
- c is the L5 code waveform of the considered signal component *XI* or *XQ*
- *NH* is the Neumann-Hoffman waveform (*NH10* if data component, *NH20* if pilot component)
- f_0 is the last intermediate frequency
- τ is the group propagation delay, θ is the received carrier phase shift (both vary over time)
- n is the additive noise

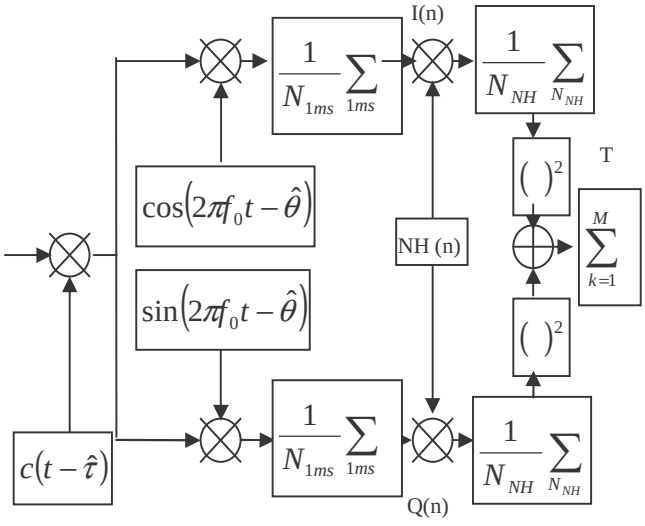

Figure 3: *NH acquisition structure.*

In the general case, the I and Q correlator outputs can be expressed as:

$$\begin{cases} I(n) = \frac{\sqrt{p}}{2}\left(\frac{\sin(\pi\Delta f T_p)}{\pi\Delta f T_p}\right) d(n)NH(n)K_c(\varepsilon_\tau)\cos(\varepsilon_\theta) \\ \quad + n_I(n) \\ Q(n) = \frac{\sqrt{p}}{2}\left(\frac{\sin(\pi\Delta f T_p)}{\pi\Delta f T_p}\right) d(n)NH(n)K_c(\varepsilon_\tau)\sin(\varepsilon_\theta) \\ \quad + n_Q(n) \end{cases}$$

where

- K_c is the L5 code auto-correlation function
- T_p is the coherent integration time (T_p=1ms in our case)
- Δf is the residual relative Doppler shift (difference between incoming carrier frequency and local carrier frequency)
- $\varepsilon_\theta = \theta - \hat{\theta}$ is the phase tracking error
- $\varepsilon_\tau = \tau - \hat{\tau}$ is the code tracking error
- n_I and n_Q are the correlator output noise samples

If we denote

- $\theta = 2\pi f_5 T(t) + \theta_0$ the phase of the incoming signal, $T(t)$ being the linear portion of the group propagation delay
- $f_{d_i} = -\frac{1}{2\pi}\frac{d\theta}{dt}$ the incoming signal Doppler shift
- $f_{d_l} = -\frac{1}{2\pi}\frac{d\hat{\theta}}{dt}$ the local signal Doppler shift
- $\Delta f = f_{d_i} - f_{d_l}$ the residual relative Doppler shift

It can be shown that in presence of residual Doppler, the correlator outputs can be expressed as:

$$\begin{cases} I(n) = \frac{\sqrt{P}}{2}\left(\frac{\sin(\pi\Delta f T_p)}{\pi\Delta f T_p}\right) d(n)NH(n)K_c(\varepsilon_\tau) \\ \quad \times\cos(2\pi\Delta f n T_p + \varepsilon_{\theta_0}) + n_I(n) \\ Q(n) = \frac{\sqrt{P}}{2}\left(\frac{\sin(\pi\Delta f T_p)}{\pi\Delta f T_p}\right) d(n)NH(n)K_c(\varepsilon_\tau) \\ \quad \times\sin(2\pi\Delta f n T_p + \varepsilon_{\theta_0}) + n_Q(n) \end{cases}$$

where

- T_p is the coherent integration time (T_p=1ms in our case).
- $\varepsilon_{\theta_0} = \theta_0 - \hat{\theta}_0$

As we can see from this expression, the correlator outputs are multiplied by *cos* and *sin* weights whose phase is varying *ms* after *ms*. The frequency of this variation is precisely the relative Doppler residual Δf. When a classical acquisition structure is used, these correlator outputs are squared and summed, removing these *cos* and *sin* weights.

In the structure proposed in [Hegarty, Tran and Van Dierendonck, 2002], these correlator outputs are multiplied by a local NH replica, then 10 or 20 samples are accumulated depending on the signal component considered. Therefore, in presence of a residual Doppler, as these weights will have changed from sample to sample, the squared sums will not remove these weights and the resulting squared correlation function will be distorted.

Considering NH20, the samples resulting from this new accumulation can be expressed as:

$$\begin{cases} I_{NH}(m) = \frac{1}{20}\sum_{n=1}^{N_{NH}} I(n)NH(n-m) \\ Q_{NH}(m) = \frac{1}{20}\sum_{n=1}^{N_{NH}} Q(n)NH(n-m) \end{cases}$$

Note that the code correlation function in presence of Doppler is different from the code correlation with zero Doppler.

To take this effect into account, a new NH code / Doppler search can be performed. In this case, the I and Q correlator samples need not only to be multiplied by a local NH code replica, but also by a local carrier. In that case, due to the *sinc* weight affecting the correlator outputs, a Doppler search must be carried out using Doppler cells.

An evaluation of the numerical impact of the Doppler residual on the acquisition criterion is proposed first.

We propose here to evaluate the effect of the Doppler residual on the direct and combined L5 code and NH20 acquisition criterion. In the first step, the direct and combined L5 code and NH20 acquisition criterion proposed in [Hegarty, Tran and Van Dierendonck**,** 2002] is evaluated in presence of Doppler residual.

In the second step, this acquisition criterion is evaluated for a complete NH20 code / Doppler search. This

search is carried out for all 20 bits of the NH20 code, and in the complete -9 kHz + 9 kHz search interval. The size of the Doppler bins is implied by the 20ms integration time inducing a *sinc* weight having its first zero in 50 Hz. In the evaluation proposed, the complete search window is [-250 Hz; 250 Hz].

In both steps, we assume that the L5 code alignment is correct within 1 ms ($\tau = \hat{\tau}$ modulo 1 ms) and no additional constant phase shift is affecting the carriers ($\theta_0 = \hat{\theta}_0$).

We analyze the evolution of the combined L5 code NH20 acquisition test criterion as a function of the local NH20 lag with different values of the residual relative Doppler shift.

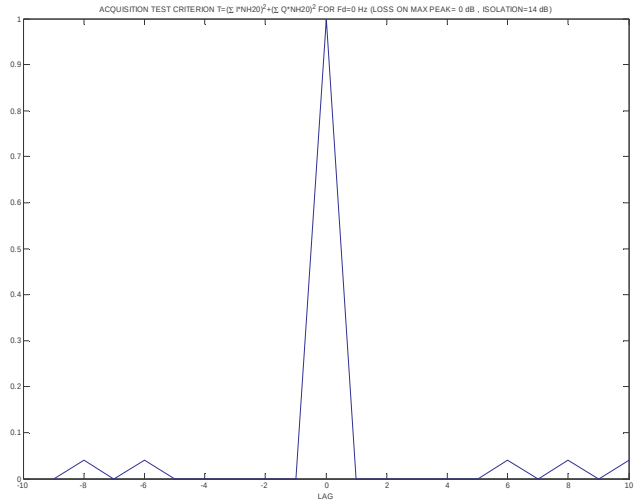

Figure 4: *Cross-correlation between 1ms correlator outputs and local NH20 (residual Doppler=0 Hz).*

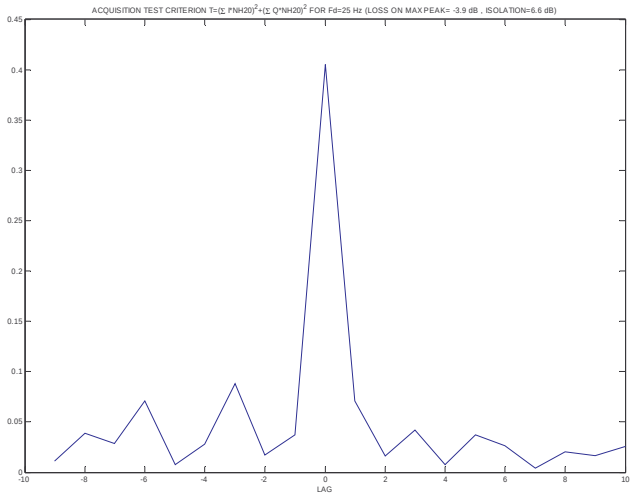

Figure 5: *Cross-correlation between 1ms correlator outputs and local NH20 (residual Doppler=25 Hz).*

Figure 4 shows the correlation function of the NH20 code in the absence of Doppler residual. We note the 14 dB isolation between the main peak and the secondary peaks.

Figure 5 shows the correlation function of the NH20 code with a Doppler residual of 25 Hz. Note that the isolation between the main peak and the secondary peaks is now only 6.6 dB.

Therefore, this direct and combined L5 code and NH20 acquisition criterion degrades quickly and does not present any useful peak when the Doppler residual is larger than 30 Hz.

We recall that in this case, we assume that the L5 code alignment is correct within 1 ms ($\tau = \hat{\tau}$ modulo 1 ms) and no additional constant phase shift is affecting the carriers ($\theta_0 = \hat{\theta}_0$).

We analyze the evolution of the combined L5 code NH20 acquisition test criterion as a function of the local NH20 lag. First of all, this test criterion is evaluated in all the Doppler bins within [-250 Hz; +250 Hz], each Doppler bin having a size of 20 Hz.

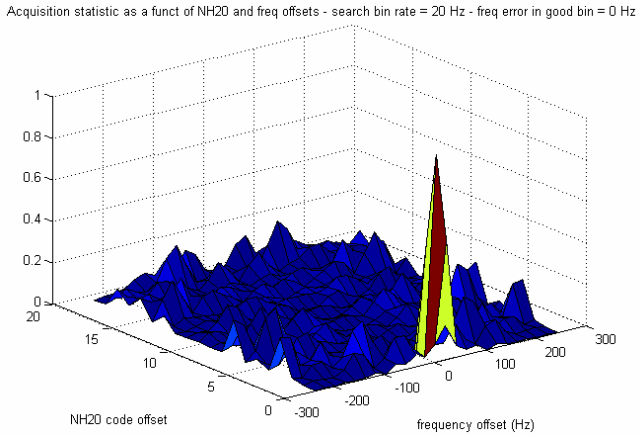

Figure 6: *3D plot of the test acquisition criterion evolution as a function of code and Doppler offsets (residual Doppler=0 Hz).*

Figure 6 shows the evolution of that criterion in presence of residual Doppler of 0 Hz. As we can see, many secondary lobes appear that could hide the main peak in presence of perturbations.

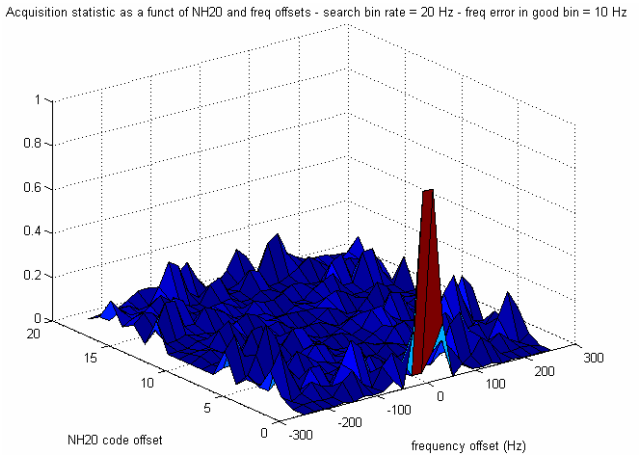

Figure 7: *3D plot of the test acquisition criterion evolution as a function of code and Doppler offsets (residual Doppler=10 Hz).*

Figure 7 shows the evolution of that criterion in presence of residual Doppler of 10 Hz. As we can see, again, many secondary lobes appear that could hide the main peak in presence of perturbations.

Then, the test criterion is evaluated in all the Doppler bins within [-250 Hz; +250 Hz], each Doppler bin having a size of 25 Hz. This search is performed so that the Doppler shift in the correct frequency bin is 12 Hz leading to the worst attenuation of the correlation peak. We then plot the superposition of that curve for all Doppler bins in figure 8.

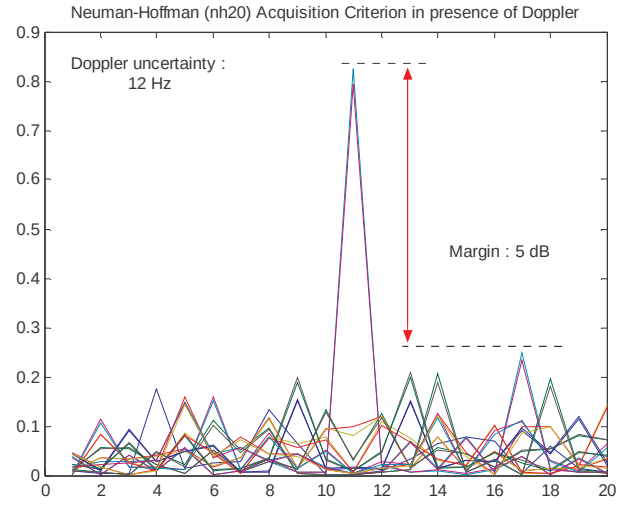

Figure 8: *Superposition of the test acquisition criterion for various Doppler offsets as a function of code lag (residual Doppler=12 Hz).*

As we can see, the acquisition criterion is again very distorted and the isolation between the main peak in the good Doppler bin and the secondary peaks in the other bins is only 4.8 dB. Note that this margin does not improve when the received L5 signal power increases.

We then searched for another 20 bit sequence that would offer good cross-correlation properties in absence and in presence of residual Doppler. We tried the sequence proposed in [Mertens, 1996]. The resulting correlation function in absence of residual Doppler exhibits the same isolation as the NH20 sequence (14 dB).

The superposition of all values of the acquisition criterion for all Doppler bins is shown in figure 9. As we can see, the isolation of the main peak in presence of Doppler is 6.8 dB.

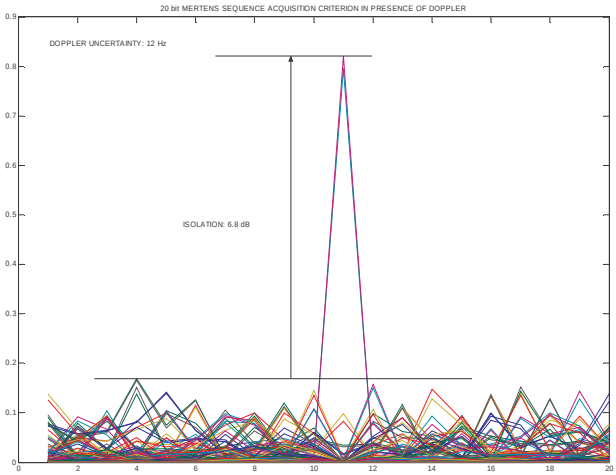

Figure 9: *Superposition of the test acquisition criterion (Mertens code) for various Doppler offsets as a function of code lag (residual Doppler=12 Hz).*

As a conclusion, according to the evaluation presented here, the direct and combined L5 code / Neumann-Hoffman acquisition criterion proposed in [Hegarty, Tran and Van Dierendonck, 2002] is highly degraded by relative Doppler residual.

Indeed, this criterion no longer exhibits a clear peak in the proper search cell as secondary lobes of the correlation function can show to be isolated only by 4.8 dB with respect to the main peak.

However, to conclude on this acquisition performance, it remains to be evaluated the exact effect of noise on this acquisition criterion in order to assess the real emergence of the peak.

IV.3. NEUMANN-HOFFMAN CODES ACQUISITION

Because of these degradations, it is necessary to determine whether it is possible to reduce the frequency uncertainty using an FLL, then perform the NH synchronization once the residual frequency error is low.

At the end of the acquisition process, one can assume a Doppler uncertainty of [-250 Hz; + 250 Hz] and a code delay uncertainty of [-0.25 T_c; +0.25 T_c].

As a consequence, it is required that the FLL used right after the acquisition process has a pull-in range of [-250 Hz; + 250 Hz]. The implemented FLL can be used easily with a predetection integration time T_p of 1ms, but use of a larger integration time requires the synchronization of the Neumann-Hoffman codes either on the data or on the pilot channel.

The performance of the FLL will be driven by the nature of correlator outputs used (data, pilot), the nature of the discriminator used, and the discriminator combination technique in case of the use of data and pilot correlator outputs.

In the case of the use of data and pilot prompt correlator outputs I_{IP}, Q_{IP}, I_{QP} and Q_{QP}, then several discriminators and combination techniques can be used to build the FLL. Examples of possible FLL discriminators for the data or the pilot channel are given here:

$$V_1(n) = \arctan\left(\frac{Q_P(n)}{I_P(n)}\right) - \arctan\left(\frac{Q_P(n-1)}{I_P(n-1)}\right) \quad \text{and}$$

$$\begin{cases} V_1(n) = V_1(n) - \pi \text{ if } V_1(n) > \frac{\pi}{2} \\ V_1(n) = V_1(n) + \pi \text{ if } V_1(n) < -\frac{\pi}{2} \end{cases}$$

$$V_2(n) = \arctan\left(\frac{I_P(n-1)Q_P(n) - I_P(n)Q_P(n-1)}{I_P(n)I_P(n-1) + Q_P(n)Q_P(n-1)}\right)$$

where *arctan(r)* is the common arctangent function returning an angle lying in $\left[-\frac{\pi}{2};\frac{\pi}{2}\right]$. Extended *arctan* discriminators are not considered here because of the presence of the Neumann-Hoffman code.

If we model the correlator outputs on the data component as

$$\begin{cases} I(n) = \frac{\sin \pi\Delta f}{\pi\Delta f} D(n)NH(n)R(\varepsilon_\tau)\cos\varepsilon_\theta + n_I(n) \\ Q(n) = \frac{\sin \pi\Delta f}{\pi\Delta f} D(n)NH(n)R(\varepsilon_\tau)\sin\varepsilon_\theta + n_Q(n) \end{cases}$$

then the output of these discriminators is

$V_1(n) = \varepsilon(n) + k_1(n)\pi - \varepsilon(n-1) - k_1(n-1)\pi + n_{V_1}(n)$ whatever the value of NH and data bits

$V_2(n) = \varepsilon(n) - \varepsilon(n-1) + k_2(n)\pi + n_{V_2}(n)$ whatever the value of NH and data bits

where

k_1 is such that $-\frac{\pi}{2} < \varepsilon(n) + k_1(n)\pi < \frac{\pi}{2}$

k_2 is such that $-\frac{\pi}{2} < \varepsilon(n) - \varepsilon(n-1) + k_2(n)\pi < \frac{\pi}{2}$

n_v is the noise affecting the discriminator tension

If we model $\varepsilon(n) = 2\pi\Delta f n T_p$, then the limit for an acceptable variation of the tracking error ε with time is given by

$-\frac{\pi}{2} < 2\pi\Delta f n T_p < \frac{\pi}{2}$ or $-\frac{1}{4T_p} < \Delta f < \frac{1}{4T_p}$ for V_1 and V_2

Therefore, at the startup of the FLL, the Doppler difference between the local and the incoming carrier should be limited to $+/-\frac{1}{4T_p}$ for V_1 and V_2. In the case where T_p=1ms, then the admissible Doppler range at the startup of the loop is [-250 Hz; +250 Hz].

We can see here that in the case of the first discriminator, jumps of π can occur in the discriminator function. In the case of the second discriminator, jumps of 2π may occur, and jumps of π or 2π may also occur if the estimated data bit is wrong. Note that these jumps do not systematically lead to the divergence of the loops. If these jumps are rare, then the loop will be able to converge anyway.

In each case, the linear loop model is the following one:

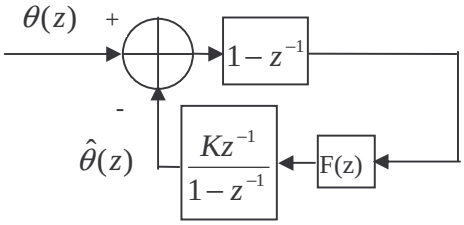

Figure 10: *FLL linear model.*

It is important to note that this model is only valid when the loop noise bandwidth is at least 10 times smaller

than the predetection bandwidth. In our case where the predetection integration time is 1ms, this means that this model is only valid when the FLL loop noise bandwidth is lower than 100 Hz. From the linear model, we see that if this is true, then using a 2nd order FLL filter *F(z)* (2nd order FLL) is enough to guarantee no tracking error in presence of a jerk of any magnitude. Thus in that case the pull-in range is as wide as the acceptable range given earlier.

The noise resistance is driven here by the loss of lock threshold, determined by the linear range of the discriminator. Here, the limit is given by the *arctan* discriminator linear range. That range is $\left[-\frac{\pi}{2};\frac{\pi}{2}\right]$ for the *arctan*.

As explained in [Kaplan, 1996], the standard deviation of the frequency estimation error is

$$\sigma_{FLL} = \frac{1}{2\pi T_p}\sqrt{\frac{8B_n}{\frac{C}{N_0}}\left(1+\frac{1}{T_p\frac{C}{N_0}}\right)} \quad \text{Hz.}$$

for an FLL.

The loss of lock threshold is such that

$$3\sigma_{PLL} < Th$$

which is equivalent to

$$\frac{C}{N_0} = \frac{36\left(\frac{1}{2\pi T_p}\right)^2 B_n}{Th^2}\left[1+\sqrt{1+\frac{Th^2}{18\left(\frac{1}{2\pi T_p}\right)^2 B_n T_p}}\right]$$

where *Th* is such that [*-Th*;*Th*] is the linear range in Hz of the discriminator.

In the case of the arctan discriminator, that range is $\left[-\frac{1}{4T_p};\frac{1}{4T_p}\right]$, therefore $Th=\frac{1}{4T_p}$. As a consequence, the loss of lock threshold is expressed as:

$$\frac{C}{N_0} = \frac{9B_n}{\pi^2}\left[1+\sqrt{1+\frac{2\pi^2}{9B_nT_p}}\right]$$

The evolution of the loss of lock threshold as a function of the FLL noise bandwidth is plotted in figure 11.

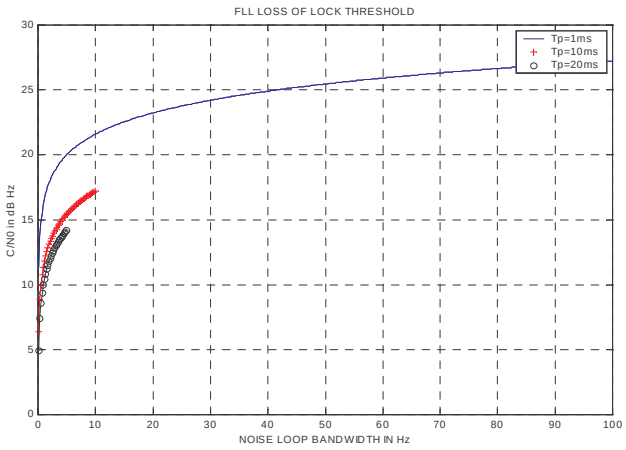

Figure 11: *FLL loss of lock threshold on a single data or pilot signal component.*

As we can see, for a FLL with a noise loop bandwidth of 10 Hz, the composite L5 signal loss of lock threshold is 24.6 dB Hz when T_p=1 ms and the composite L5 signal loss of lock threshold is 20.2 dB Hz when T_p=10ms.

The FLL loss of lock threshold for T_p=1ms and B_n=10 Hz is thus around 25 dB Hz for the composite L5 signal, which is well under the acquisition threshold (33.7 dB Hz). Therefore, that simple FLL can be used right after the acquisition process.

If the FLL is to be used at a C/N_0 lower than 25 dB Hz, then either the noise bandwidth must be reduced or the integration time must be increased.

V. TRACKING PERFORMANCE

ATAN AND EXTENDED ATAN DISCRIMINATORS COMBINATION

The possible PLL discriminators are the following ones:

$$V_1(n) = \arctan\left(\frac{Q_P(n)}{I_P(n)}\right)$$

$$V_2(n) = \arctan\left(Q_P(n), I_P(n)\right)$$

where

arctan(r) is the common arctangent function returning an angle lying in $\left[-\frac{\pi}{2};\frac{\pi}{2}\right]$

arctan(y,x) is the extended arctangent function returning an angle lying in $[-\pi;\pi]$.

After *NH20* synchronization, any of these 2 discriminators can be applied with the pilot channel correlator outputs. The use of the extended *arctan* discriminator on the data channel would require the estimation of the data bit from the correlator outputs, then a correction of the correlator outputs before they can be used to form a discriminator function.

If we model the correlator outputs as

$$\begin{cases} I(n) = \dfrac{\sin \pi \Delta f}{\pi \Delta f} D(n) NH(n) R(\varepsilon_\tau) \cos \varepsilon_\theta + n_I(n) \\ Q(n) = \dfrac{\sin \pi \Delta f}{\pi \Delta f} D(n) NH(n) R(\varepsilon_\tau) \sin \varepsilon_\theta + n_Q(n) \end{cases}$$

then the output of these discriminators is

$V_1(n) = \varepsilon(n) + k_1(n)\pi + n_{V_1}(n)$ whatever the presence and the value of data bits

$V_2(n) = \varepsilon(n) + 2k_2(n)\pi + n_{V_2}(n)$ if the data bits are not present or properly estimated

where

k_1 is such that $-\dfrac{\pi}{2} < \varepsilon(n) + k_1(n)\pi < \dfrac{\pi}{2}$

k_2 is such that $-\pi < \varepsilon(n) + 2k_2(n)\pi < \pi$

n_v is the noise affecting the discriminator tension

Each of these individual discriminator functions in the data and in the pilot channel can be combined to form a composite discriminator function used to drive the carrier NCO [Hegarty, 1999], [Tran and Hegarty, 2002]. The combination can be a simple average or a more complex weighted sum depending on the prior knowledge of the noise power affecting each discriminator output such as modelled here:

$$V(n) = \frac{\alpha_1}{\alpha_1 + \alpha_2} V_1^{data}(n) + \frac{\alpha_2}{\alpha_1 + \alpha_2} V_1^{pilot}(n)$$

When implementing this type of combination, one must take care to the jumps in *V(n)* that may arise from a steady-state tracking error due to range dynamics inducing a wrapping of one individual discriminator.

For example, we can build a composite discriminator function by combining a classical *arctan* discriminator on the data channel with a classical *arctan* discriminator on the pilot channel. In this case, in the presence of large dynamics, a bias will be present at the output of each discriminator and jumps of π may arise from each individual discriminator due to the limited range of the classical *arctan*, resulting in no bias for the composite discriminator. In presence of noise only, the tracking threshold will be driven by the acceptable noise power in the operating range of the classical *arctan* function.

In order to take benefit from the absence of data on the pilot channel, one may desire to form a composite discriminator function by combining a classical *arctan* on the data channel with an extended *arctan* on the pilot channel. In that case, to benefit from the full operating range of the extended *arctan*, it is necessary to detect and correct the possible jumps of π that may arise from the classical *arctan* discriminator in the presence of large dynamics. A possible technique to do this is to run a step detection procedure on the difference of the data discriminator and pilot discriminator.
The proposed test criterion is thus

$$V(n) = V_1^{data}(n) - V_2^{pilot}(n)$$

The average value of the test criterion is zero when the *arctan* discriminator is not affected by a step. We can assume that each discriminator is affected by independent noise as it originates from the correlation of the incoming signal with different PRN codes. Therefore, the variance of the test criterion is the sum of the variance of each discriminator which is taken here to be

$$\sigma_{PLL} = \sqrt{\frac{B_n}{\dfrac{C}{N_0}} \left(1 + \frac{1}{2T_p \dfrac{C}{N_0}} \right)}$$

An example step detection procedure is a CUSUM test [Basseville and Nikiforov, 1993]. That CUSUM test could be designed to test changes in the average value of the test criterion, modelling the test criterion as a white Gaussian noise with standard deviation σ_V such that

$$\sigma_V = \sqrt{2 \frac{B_n}{\dfrac{C}{N_0}} \left(1 + \frac{1}{2T_p \dfrac{C}{N_0}} \right)}$$

Important design parameters of this CUSUM test are the false alarm rate P_{fa}, the missed detection rate P_{md}, and the time to alert T_A. When the design false alarm rate tends to 0, it can be shown that the smallest detectable bias is equal to $b = \sqrt{\dfrac{2\sigma_\varepsilon^2}{T_A} \left(h_D + \alpha \sqrt{2h_D} \right)}$ where h_D is the test threshold $h_D = \ln\left(\dfrac{2}{P_{fa}} \right)$ and $\alpha = \sqrt{2} ERFINV(1 - 2P_{md})$. The following figure shows the lowest C/N_0 required to guarantee the performance of the CUSUM procedure as a function of the

loop noise bandwidth when the predetection time is set equal to 10 ms:

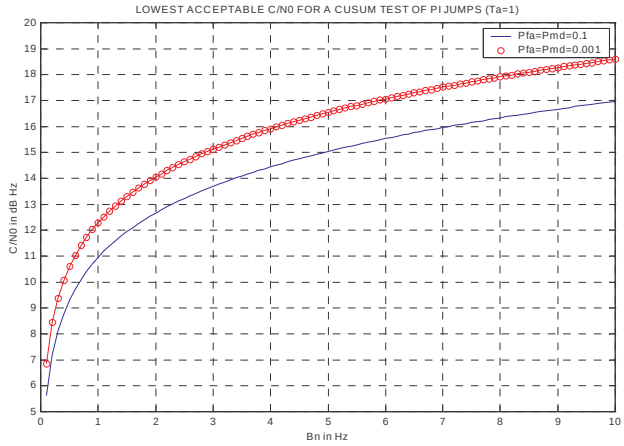

Figure 12: *Lowest acceptable data or pilot channel C/N_0 as a function of loop noise bandwidth to test for pi jumps in the classical arctan discriminator when Tp=10 ms.*

That lowest C/N_0 for efficient detection can be compared to the tracking threshold of a loop using a composite discriminator formed using classical *arctan* discriminators on the data and pilot channels. The standard deviation of an *arctan* PLL is

$$\sigma_{PLL} = \sqrt{\frac{B_n}{\frac{C}{N_0}}\left(1+\frac{1}{2T_p\frac{C}{N_0}}\right)}$$

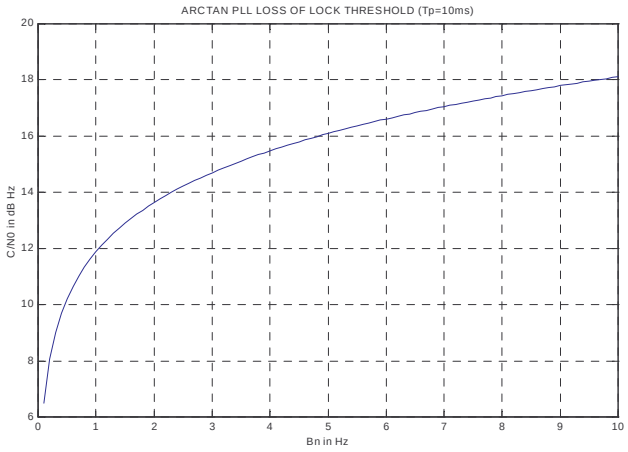

Figure 13: *Arctan PLL loss of lock threshold (composite data+pilot L5 signal C/N_0) as a function of PLL equivalent noise bandwidth.*

It is also interesting to determine the tracking threshold of an extended *arctan* loop tracking only the pilot signal component. That tracking threshold is plotted in figure 13.

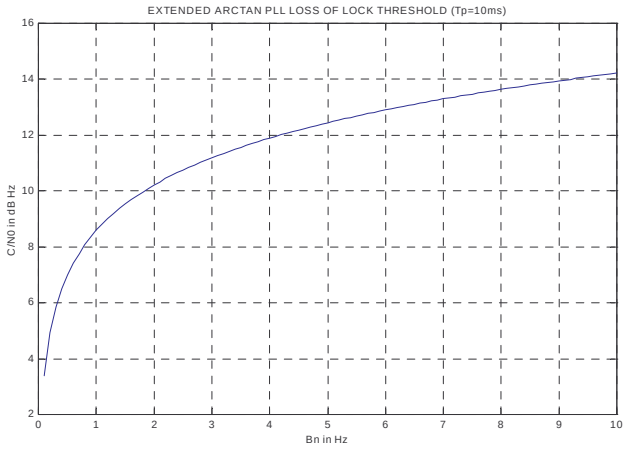

Figure 14: *Extended arctan PLL loss of lock threshold (pilot L5 signal C/N_0) as a function of PLL equivalent noise bandwidth.*

As we can see from the comparison of figures 11 and 12, when T_p=10ms, the composite data+pilot L5 signal C/N_0 threshold for detection of the pi jumps is larger than the loop tracking threshold for a classical *arctan* discriminator. In addition, from figure 14, the composite data+pilot L5 signal C/N_0 loss of lock threshold of an extended *arctan* PLL using only the pilot component is lower than the above two thresholds. Therefore, the utility of the implementation of hybrid discriminator functions is questionable and does not seem to bring a possible gain with respect to the implementation of a simple extended *arctan* PLL on the pilot L5 component.

It must also be noted here that each individual discriminator function could be combined at the output of 2 different loop filters. The data discriminator could be taken at the output of a much tighter loop filter than the pilot discriminator. In that way, the data loop filter could compensate for the larger noise affecting the data discriminator. Other possibilities include the computation of products of I and Q samples of the data correlator outputs before further accumulation and combination with pilot discriminator.

Finally, the combination of data and pilot correlator outputs to drive the DLL is not affected by jumps due to the nature of DLL discriminators, and therefore represents a real interest to reduce the code tracking threshold.

CONCLUSION

There is a 2dB benefit in the acquisition of L5 codes by using correlator outputs jointly from data and pilot components. There is a limitation to 1ms in the duration of the coherent integration due to the Neumann-Hoffman codes which is small compared to the 20 ms limitation in the L1 GPS C/A signal.

Direct and combined L5 codes and Neumann-Hoffman codes acquisition criterion is highly degraded in presence of residual Doppler (peak isolation = 5 dB for NH20, peak isolation = 7 dB for 20 bit Mertens code). The real performance of this acquisition remains to be assessed.

Neumann-Hoffman codes can be acquired after reduction of the residual frequency error using an FLL that was shown to have a tracking threshold lower than the L5 codes acquisition threshold.

Combination of atan and extended atan discriminators in the L5 PLL is affected by jumps and does not provide the expected gain in the phase tracking threshold compared to a pure PLL using only pilot correlator outputs.

ACKNOWLEDGMENTS

The authors would like to acknowledge the assistance of Neila Kraiem and Nicolas Sacco who searched for other short PRN sequences, as well as Anne-Laure Morisseau and Fatou Gueye for the analysis of the L5 signal.

REFERENCES

[Basseville and Nikiforov, 1993], M. BASSEVILLE, I. NIKIFOROV, **« Detection of Abrupt Changes: Theory and Application”**, Prentice Hall, 1993

[Bastide et al., 2002], F. BASTIDE, O. JULIEN, C. MACABIAU, B. ROTURIER, **« Analysis of E5/L5 acquisition, tracking and data demodulation thresholds”**, ION GPS 2002

[Hegarty., 1999], C. HEGARTY, **« Evaluation of the proposed Signal Structure for the New Civil GPS Signal at 1176.45 MHz”**, The MITRE Corporation, Working Note WN99W34, June 1999

[Hegarty, Tran and Van Dierendonck, 2002], C. HEGARTY, M. TRAN and A.J. VAN DIERENDONCK, **“Acquisition Algorithms for the GPS L5 signal”**

[Kaplan., 1996], E. KAPLAN, **« GPS Principles and Applications”**, Artech House

[Macabiau et al., 2002], C. MACABIAU, V. CALMETTES, W. VIGNEAU, L. RIES, J-L. ISSLER **« L5 Codes Properties”**, GNSS’2002

[RTCA, 2000], RTCA SC-159 **« NAVSTAR GPS L5 Signal Specifications”**

[Mertens, 1996], S. MERTENS **« Exhaustive Search for Low Autocorrelation binary Sequences”**, Institute Auto-von-guericke-universitat, Magdeburg, Letter to the Editor.

[RTCA, 2000], RTCA SC-159 **« NAVSTAR GPS L5 Signal Specifications”**

[Spilker and Van Dierendonck., 1999], J. SPILKER, A.J. VAN DIERENDONCK, **« Proposed New Civil GPS Signal at 1176.45 MHz”**, ION GPS 1999

[Tran and Hegarty., 2002], M. TRAN, C. HEGARTY, **« Receiver Algorithms for the New Civil GPS Signals”**, ION NTM 2002

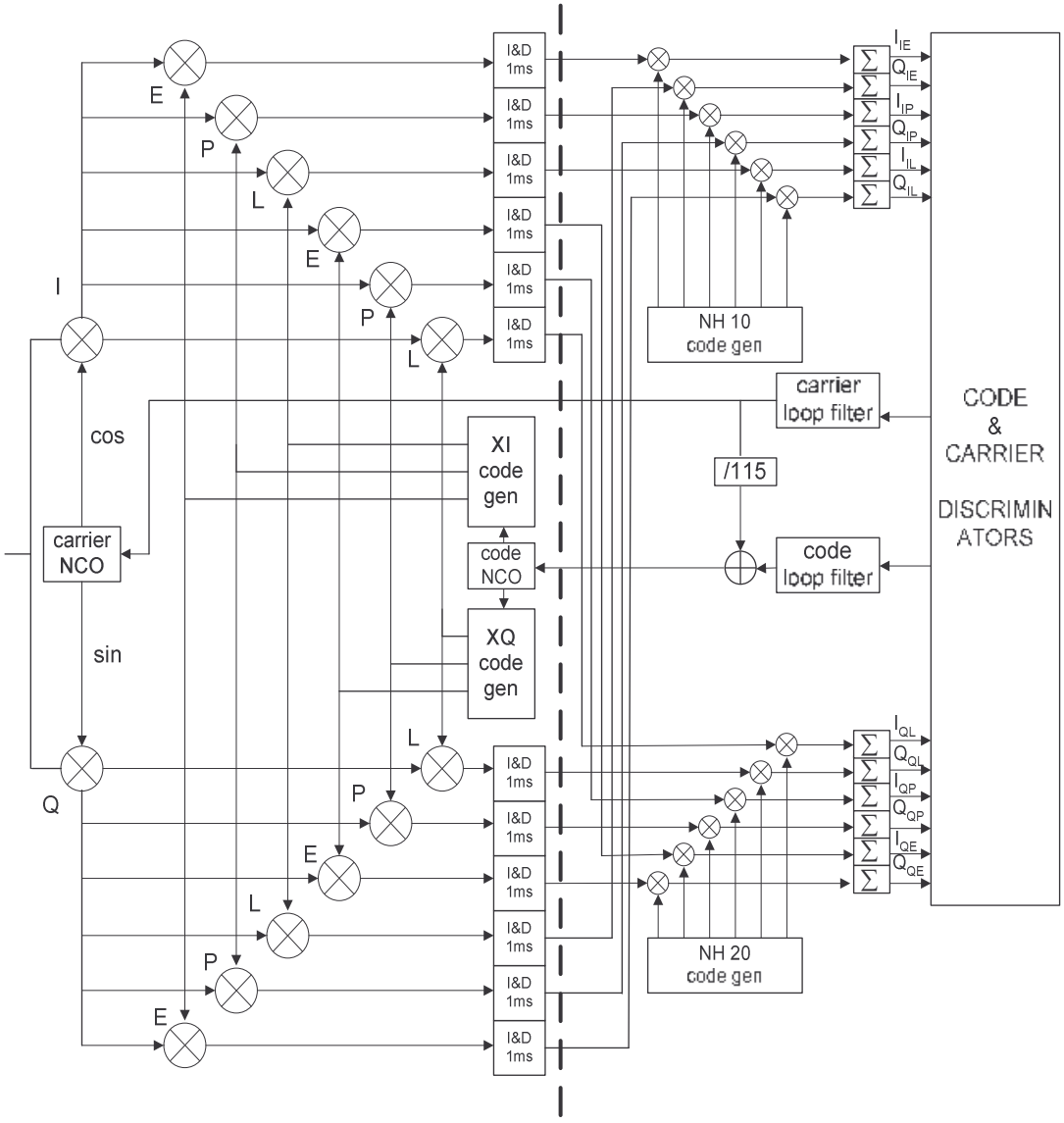

Figure 1: *Proposed L5 tracking loops structure.*